

# Receptor-Mediated Cellular Uptake of Nanoparticles: A Switchable Delivery System

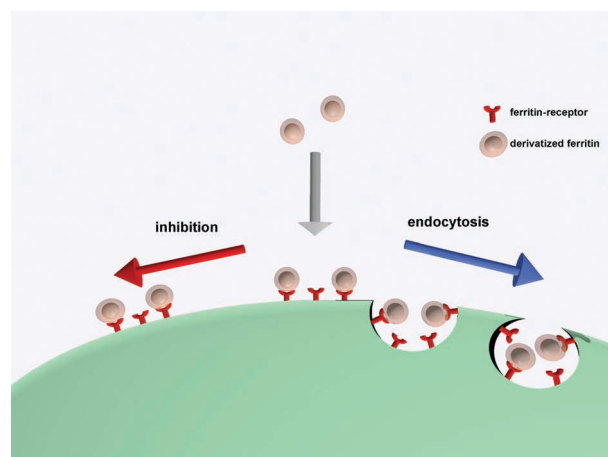
Lianbing Zhang,\* Wiebke Fischer, Eckhard Pippel, Gerd Hause, Matthias Brandsch, and Mato Knez\*

The small size of nanoparticles and nanocages enables them to overcome various biological barriers and enter target cells, which is an attractive feature for various applications in biomedicine. For example, quantum dots, gold, and magnetic nanoparticles have been used as delivery carriers for small-interference RNA (siRNA), which has been applied for silencing specific genes *in vitro* and *in vivo*.<sup>[1–3]</sup> Recently, mesoporous silica nanoparticles were proposed as ideal drug-delivery carriers in tumor therapy.<sup>[4–6]</sup> However, undesired cytotoxic effects and cellular responses, triggered by inorganic nanomaterials, remain a major challenge for *in vivo* applications.<sup>[7,8]</sup> Upon cellular uptake, interactions of nanoparticles with cellular components, for example, membranes, proteins, and DNA, can significantly contribute to the toxicity.<sup>[9–11]</sup> Moreover, new investigations frequently reveal undesired effects of materials that were once regarded as promising and safe. In 2009, Park et al. demonstrated that porous silica nanoparticles were biodegradable *in vivo* and excellently biocompatible and a use for *in vivo* tumor imaging was proposed.<sup>[12]</sup> One year later, however, Huang et al. demonstrated that mesoporous silica nanoparticles can promote tumor growth *in vivo* due to their ability to decrease cellular reactive oxygen species (ROS).<sup>[13]</sup> Aside from the generated intracellular toxicity, toxic ion leakage and remote toxicity can also be induced by extracellular inorganic nanocarriers.<sup>[8,14]</sup> Therefore, it is of great importance to develop a biocompatible carrier system that allows investigations addressing intra- and extracellular toxicity.

Compared with synthetic carriers, biological ones, such as apoferritin, show obvious superiority with regard to biocompatibility. Being the demineralized form of the iron-storage protein ferritin, apoferritin is a globular protein with an outer diameter of 12 nm and an internal cavity of 7.6 nm. Distributed around the sphere, there are 14 small channels, each 3–4 Å in diameter, perforating the protein shell and providing size selectivity for ions or molecules to enter the interior

cavity.<sup>[15]</sup> In various studies, apoferritin has already served as template for the preparation of various nanoparticles.<sup>[16–18]</sup> Our previous work has demonstrated that apoferritin could be of special interest for biomedical applications of nanoparticles as ferritin receptors, which are present on many cell membranes, allow biological cellular uptake and biomimetic application of platinum nanoparticles.<sup>[18]</sup> However, there are further benefits of apoferritin being a carrier for nanoparticles that have not been studied in detail. One of these benefits is the fact that ferritin is internalized into the cell by receptor-mediated endocytosis, which is induced by the assembly of peptide 2 (AP2)-/clathrin.<sup>[19,20]</sup> This assembly, and thus the endocytosis, can be reversibly inhibited in various ways,<sup>[19–22]</sup> offering the potential for switchable cellular uptake. As illustrated in **Scheme 1**, the combination of apoferritin, ferritin receptor, and an appropriate cell line allows control of the cellular uptake of the nanoparticles in a natural and harmless way, thus enabling *in vitro* both an investigation of the intracellular effects of nanoparticles upon cellular uptake and an extracellular investigation with the inhibition, respectively.

In this Communication, such control of the delivery system was tested on human intestinal epithelial Caco-2 cells. These cells exhibit appropriate ferritin receptors that can mediate the endocytosis. Similar to the procedure in our previous work,<sup>[18]</sup> we prepared inorganic nanoparticles within the internal cavity of horse spleen apoferritin, however, with a different composition.



**Scheme 1.** Schematics of binding and cellular uptake of ferritin-based composites. Cellular uptake via receptor-mediated endocytosis can be inhibited.

L. Zhang, Dr. E. Pippel, Dr. M. Knez  
Max Planck Institute of Microstructure Physics  
Weinberg 2, 06120 Halle, Germany  
E-mail: lianbing@mpi-halle.de; mknez@mpi-halle.de  
W. Fischer, Dr. G. Hause, Dr. M. Brandsch  
Biozentrum, Martin-Luther-University Halle-Wittenberg  
06120 Halle, Germany

DOI: 10.1002/sml.201100238

We produced PtAu alloy nanoparticles (PtAu–apo), which showed an enhanced activity towards hydrogen peroxide decomposition in comparison to the earlier described apoferritin-encapsulated platinum nanoparticles (Pt–apo). Tests on Caco-2 cells showed that upon cellular uptake, PtAu–apo is a better mimic of cellular antioxidative enzymes, reducing the externally induced ROS generation and enhancing the viability of the cells even more than Pt–apo. As a negative reference, the native ferritin, containing a ferrihydrite core, promoted the intracellular ROS generation and lowered the viability of the cells under oxidative stress. In further experiments, inhibition of endocytosis, in our case with chlorpromazine or sucrose, diminished the protective or toxic effects of the apoferritin-encapsulated nanoparticles on cells by preventing their cellular uptake. This demonstrates that apoferritin, ferritin receptors, and a cell-culture system, in combination with certain endocytosis inhibitors, can indeed compose a flexible and controllable system for investigations of the cytotoxicity of nanoparticles.

PtAu nanoparticles with an average size of  $\approx 3$  nm were prepared within apoferritin with a solution containing 250 mM  $K_2PtCl_4$  and 2.5 mM  $HAuCl_4$ . The lattice spacing of 0.230 nm was measured with a high-resolution transmission electron microscopy (HRTEM) system (FEI TITAN 80-300) and is consistent with the value expected for a PtAu alloy.<sup>[23]</sup> Further characterization with energy-dispersive X-ray (EDX) analysis demonstrated that the particles with a diameter of  $\approx 3$  nm were composed of  $\approx 50\%$  Au and 50% Pt (atomic ratio), as shown in Figure S1 of the Supporting Information (SI). An analysis by polyacrylamide-gel electrophoresis showed that the protein content of apoferritin, PtAu–apo, as well as Pt–apo and Au–apo, which were used as reference materials, showed no difference before the application of the activity assay (Figure S2 in the SI). The catalytic activity of the PtAu–apo was compared with the activity of Pt–apo prepared from 300 mM  $K_2PtCl_4$  and Au–apo prepared from 25 mM  $HAuCl_4$  (Figure 1). The  $H_2O_2$ -decomposition activity of the PtAu–apo

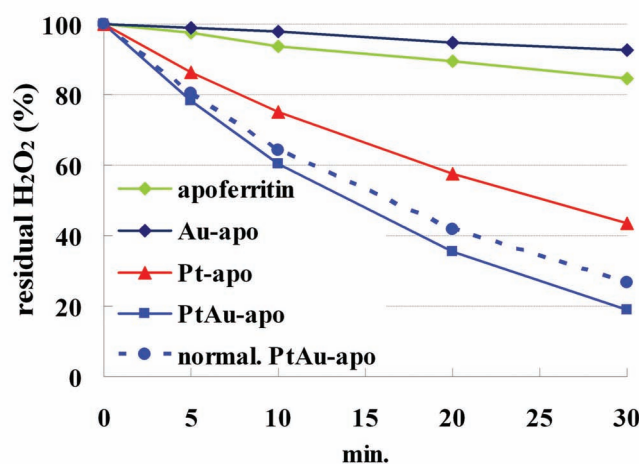


**Figure 1.**  $H_2O_2$ -decomposition activities of PtAu–apo prepared from 250 mM  $K_2PtCl_4$  and 2.5 mM  $HAuCl_4$ , Pt–apo prepared from 300 mM  $K_2PtCl_4$ , and Au–apo prepared from 25 mM  $HAuCl_4$ . For better comparison, the activity of PtAu–apo was normalized (normal Pt–apo) with the Pt content of Pt–apo by considering atomic absorption spectroscopy (AAS) results.

was higher than that of the Pt–apo, which was further confirmed after the activity of the PtAu–apo was normalized to the Pt content of Pt–apo. The Pt content was determined with atomic absorption spectroscopy (AAS), as detailed in Table S1 in the SI. The reference with Au only (Au–apo) showed no activity for the decomposition of  $H_2O_2$ , clearly demonstrating that the enhancement of the activity with PtAu–apo cannot be attributed to a combination of two individual catalysts but rather to an enhanced catalytic efficiency of the binary PtAu component. Since apoferritin is very stable in a broad pH region, the pH dependence of the decomposition reaction with PtAu–apo at pH 5.5, 7.4, and 8.3 was evaluated. The activity of PtAu–apo increased in line with increasing pH values. At pH 8.3, the PtAu–apo decomposed the  $H_2O_2$  almost completely within 30 min, while, in comparison, with Pt–apo  $>30\%$   $H_2O_2$  still remained (Figure S3 in the SI).

Once internalized into cells, the highly active PtAu–apo is expected to mimic the biological enzymes catalase and superoxide dismutase (SOD) better than Pt–apo and to help the cells to eliminate ROS and survive under oxidative stress. The native ferritin was added as further reference and toxic counterpart to PtAu–apo, since, under nonphysiological conditions, iron is released from the ferritin's ferrihydrite core, which can catalyze the production of free radicals.<sup>[24]</sup> Thus, for evaluation of the initial effects that the ferritin-based components induce upon cellular uptake, Caco-2 cells were treated with either apoferritin, ferritin, Pt–apo, or PtAu–apo, followed by a treatment with 2 mM  $H_2O_2$  to induce oxidative stress. The resulting generation of intracellular ROS by the Caco-2 cells was determined with a 2',7'-dichlorofluorescein (DCF) assay.<sup>[25]</sup> As expected,  $H_2O_2$  induced a ROS generation in Caco-2 cells treated with apoferritin, Pt–apo, or PtAu–apo that was significantly lower than that in untreated cells (Figure 2). Although

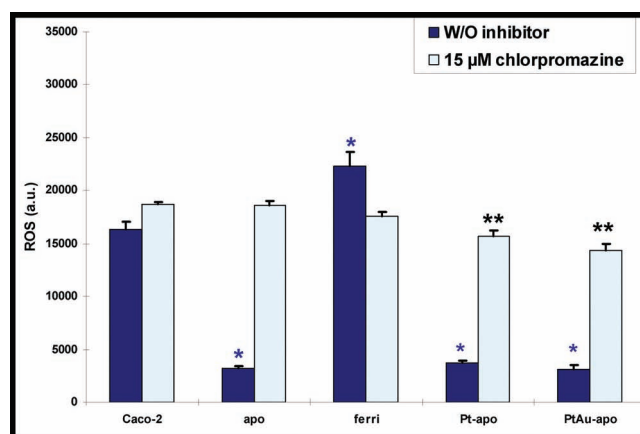


**Figure 2.** Comparison of the effects of apoferritin (apo), ferritin (ferri), Pt–apo, and PtAu–apo on the ROS generation of Caco-2 cells stressed with 2 mM  $H_2O_2$ . Inhibition of endocytosis with 15  $\mu$ M chlorpromazine significantly reduces the differences of the intracellular ROS generation. The results are presented the mean  $\pm$  standard deviation (SD) of  $n$  measurements for  $n \geq 4$ . Values marked with an asterisk are significantly different to the control (Caco-2) without inhibitor. Values marked with two asterisks are significantly different to the control with 15  $\mu$ M chlorpromazine as the inhibitor. Differences were statistically analyzed with the nonparametric two-tailed U-test and a  $p$ -value of less than 0.05 was considered significant.

apoferritin exhibits less activity against  $H_2O_2$  and superoxide, it has been observed that an overexpression of apoferritin enhanced the cellular resistance against  $H_2O_2$ -induced oxidative stress.<sup>[26,27]</sup> The proposed mechanism is that apoferritin may trap iron ions in its cavity and thus keep them unavailable for intracellular ROS generation.<sup>[28]</sup> This is different from the possible principle of effect of Pt- and PtAu-apo composites that can directly decompose  $H_2O_2$  and scavenge superoxides. The intracellular ROS level after treatment with apoferritin, Pt-apo, and PtAu-apo exhibited little difference, which may be due to the detection limit of our equipment or the short testing period. In contrast, ferritin promoted ROS generation. A high level of intracellular ROS may result in organellar damage or even cell death.<sup>[7,29]</sup> Therefore, investigation of the viability of the cells was performed and revealed that the cells profited from the negative effect of Pt-/PtAu-apo on the ROS generation: the viability of the cells under oxidative stress, externally induced with 5 mM  $H_2O_2$ , increased significantly with a treatment with Pt-/PtAu-apo composites, with the higher activity of PtAu-apo compared to Pt-apo in solution being maintained even after cellular uptake (Figure 3). Apoferritin could reduce intracellular ROS, however, this effect did not reflect on the viability. Compared with the control cells, there was no significant increase of cell viability. As already mentioned in our previous work, ROS may not be the only effect with an impact on the viability under experimental conditions.<sup>[18]</sup> In contrast, the enhanced intercellular ROS production with ferritin resulted in a significantly lower viability. This toxic effect of ferritin is in agreement with previous reports and supports the observation that ferritin together with  $H_2O_2$  causes DNA damage.<sup>[24,30]</sup>

If the cellular internalization of apoferritin-encapsulated materials does in fact take place through endocytosis, the inhibition of endocytosis will prevent the cellular uptake of both Pt-/PtAu-apo and ferritin and eliminate their respective

effects on cells. The AP2-/clathrin-dependent endocytosis can be inhibited with chlorpromazine, which prevents the formation of coated pits on the cell membrane.<sup>[22]</sup> We added a maximum of 15  $\mu$ M chlorpromazine to the incubation medium, since a higher concentration was observed to cause cell detachment. Subsequently, we proceeded with the DCF assay. As envisioned, the inhibition of the endocytosis diminished both the positive effect of Pt-/PtAu-apo and the negative effect of ferritin on the intracellular ROS generation (Figure 2). Compared with the DCF results without inhibition, the initially large differences between the components in their ROS concentration are greatly reduced. A slightly reduced intracellular ROS level after the inhibition of endocytosis was observed in cells treated with Pt-apo and PtAu-apo. The explanation may be as simple as the following: since such inhibition does not prevent the binding of Pt/PtAu-apo to the receptors, Pt-/PtAu-apo bound to the cell surface can still decompose extracellular  $H_2O_2$  and thus reduce the  $H_2O_2$  concentration. Obviously, this extracellular activity of Pt/PtAu-apo has a minor effect on the intracellular ROS. The diminished negative effect of ferritin also indicates that ferritin does not affect cellular ROS through a direct reaction with  $H_2O_2$ . In addition, toxic ion leakage from ferritin outside the cells appears to be of no significance.

Similarly to the DCF-assay tests, the toxic effect of ferritin as well as the positive effect from Pt-/PtAu-apo on the viability was eliminated when chlorpromazine was used as endocytosis inhibitor (Figure 3). Besides chlorpromazine, a medium with 450 mM sucrose was used to inhibit endocytosis through hyperosmosis.<sup>[19-21]</sup> Similar results to those with chlorpromazine as inhibitor were obtained. The viability of the cells exhibited no significant variation upon treatments with either of those inhibitors. Together with the DCF assay, the effects of PtAu-apo of reducing the intracellular ROS and increasing the viability were confirmed. The minor effects the extracellular Pt/PtAu-apo have on the ROS showed no significant impact on the viability, indicating that the intracellular ROS is not the only source of toxicity involved. The results demonstrated that the cellular uptake of apoferritin-encapsulated materials is based on receptor-mediated endocytosis. Through this pathway, apoferritin can deliver both toxic and nontoxic or even supporting materials into cells, which can be controlled by the inhibition of endocytosis.

In summary, binary PtAu nanoparticles were synthesized within apoferritin. This protein nanosphere can serve as a natural and biocompatible carrier for cellular delivery of bioactive materials through receptor-mediated endocytosis. Cellular tests demonstrated that this biocompatible carrier enables the cellular delivery of both toxic components (e.g., ferritin) and catalytically active PtAu, which can be potentially applied in a biological environment, for example, as an enzyme mimic to support cells under oxidative stress (Figure S4 in the SI). The apoferritin, the ferritin receptor, and appropriate cells constitute a simple system for in vitro cellular investigation of intra- and extracellular effects of inorganic materials. The possibility of preventing cellular uptake by the inhibition of endocytosis makes this system very flexible and highly practical, for example, for the investigation of cytotoxicity caused by ion leakage. The system is

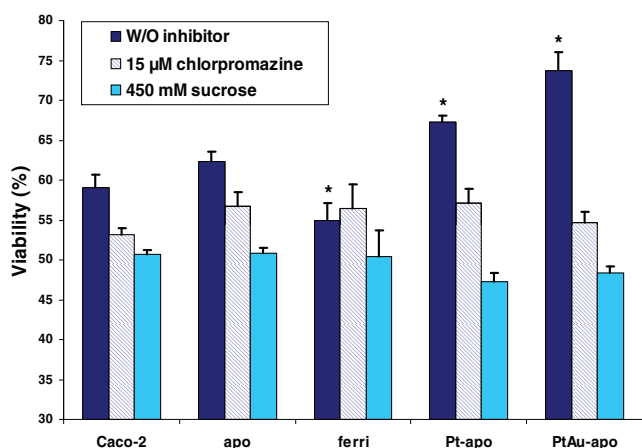


**Figure 3.** Effects of apoferritin (apo), ferritin (ferri), Pt-apo, and PtAu-apo on the viability of Caco-2 cells stressed with 5 mM  $H_2O_2$  and without inhibition of endocytosis. The viability of unstressed cells was set to be 100%. Inhibition of endocytosis with chlorpromazine or sucrose eliminates the differences between the effects. The results are presented as the mean  $\pm$  SD for  $n \geq 4$ . Values marked with an asterisk are significantly different to the control (Caco-2) without inhibitor. Statistical analysis was done with the nonparametric two-tailed U-test and a  $p$ -value of less than 0.05 was considered significant.

superior to common incorporation of inorganic nanoparticles through cell membranes as it offers a nondestructive (to the cell membrane) as well as switchable method of cellular uptake, allowing more precise investigations of cytotoxicity of various inorganic nanomaterials on a plethora of cell types, since a large number of cells contain ferritin receptors and can be treated in a similar way.<sup>[19,20]</sup>

## Experimental Section

**Cell Culture:** The human colon adenocarcinoma cell line Caco-2 was obtained from the German Collection of Microorganisms and Cell Cultures. Cells (passages 22–26) were cultured in minimum essential medium (MEM; PAA Laboratories, Germany) supplemented with 10% fetal bovine serum (FBS) (Biochrom), 1% nonessential amino acids and 50 mg mL<sup>-1</sup> gentamicin (PAA).

For the assays, Caco-2 cells at 80–90% density were released using trypsin/EDTA (ethylenediaminetetraacetate, Sigma-Aldrich, Germany) (0.05%/0.02%) and seeded onto disposable nonfluorescent 24- or 96-well plates at a density of  $0.75 \times 10^5$  cells cm<sup>-2</sup> and cultured for 12 d. The culture medium was replaced 1 d after seeding, then every 2 d, and 1 d before the assay.

**Determination of Intracellular ROS:** The intracellular ROS in Caco-2 cells was determined by intracellular oxidation of nonfluorescent 2',7'-dichlorodihydrofluorescein (DCFH) to fluorescent DCF. Cells were incubated with the culture medium with or without apoferritin, ferritin, or Pt-apo and PtAu-apo for 1 h at 37 °C. The cells were then washed two times with phosphate-buffered saline (PBS) and incubated with 20 μM DCFH diacetate (DCFH-DA) in PBS for 10 min in the dark. After uptake by the cells, DCFH-DA was hydrolyzed to DCFH by intracellular esterase. After rinsing twice with PBS, the cells were incubated with 2 mM H<sub>2</sub>O<sub>2</sub> in PBS for 45 min. The net changes of the intracellular level of the reactive oxygen species were determined by measuring the fluorescence of DCF before and after the H<sub>2</sub>O<sub>2</sub> treatment at wavelengths of 485 nm (excitation) and 520 nm (emission) with a microplate reader (FLUOstar Galaxy, BMG Labtech, Offenburg). Each sample was run in triplicate with background control.

**Determination of the Cell Viability:** For the determination of the cell viability, a Cell-Counting Kit 8 (CCK-8) (Sigma-Aldrich) was used. Briefly, after the incubation with apoferritin, ferritin, Pt-apo, and PtAu-apo for 1 h at 37 °C, the cells were washed twice with PBS and treated with 5 mM H<sub>2</sub>O<sub>2</sub> in the culture medium without FBS for 45 min. The cells were then washed twice with PBS and incubated in the culture medium with 10% CCK-8 solution for 2 h. The viability was determined by measuring the absorbance at 450 nm using a microplate reader (FLUOstar Galaxy, BMG Labtech, Offenburg). Each sample was run in triplicate with background control.

**Inhibition of Endocytosis:** For the inhibition, MEM with 15 μM chlorpromazine or 450 mM sucrose was used during incubation with apoferritin, ferritin, Pt-apo, and PtAu-apo. The following ROS and viability determination was carried out with normal MEM.

## Supporting Information

Supporting Information is available from the Wiley Online Library or from the author.

## Acknowledgements

The authors gratefully acknowledge the financial support of the German ministry of education and research (BMBF) under the contract number 03 × 5507 and the international Max Planck Research School for Science and Technology of Nanostructures (Nano-IMPRS), and Deutsche Forschungsgemeinschaft grant #BR 2430/1–2.

- [1] K. A. Whitehead, R. Langer, D. G. Anderson, *Nat. Rev. Drug Discov.* **2009**, *8*, 129.
- [2] N. Singh, A. Agrawal, A. K. L. Leung, P. A. Sharp, S. N. Bhatia, *J. Am. Chem. Soc.* **2010**, *132*, 8241.
- [3] K. Nishina, T. Unno, Y. Uno, T. Kubodera, T. Kanouchi, H. Mizusawa, T. Yokota, *Mol. Ther.* **2008**, *16*, 734.
- [4] I. Slowing, B. G. Trewyn, V. S. Lin, *J. Am. Chem. Soc.* **2006**, *128*, 14792.
- [5] J. Qian, A. Gharibi, S. He, *J. Biomed. Opt.* **2009**, *14*, 014012.
- [6] J. Lu, M. Liong, J. I. Zink, F. Tamanoi, *Small* **2007**, *3*, 1341.
- [7] Y. Pan, A. Leifert, D. Ruau, S. Neuss, J. Bornemann, G. Schmid, W. Brandau, U. Simon, W. Jahnen-Dechent, *Small* **2009**, *5*, 2067.
- [8] N. Lewinski, V. Colvin, R. Drezek, *Small* **2008**, *4*, 26.
- [9] B. Wang, L. Zhang, S. C. Bae, S. Granick, *Proc. Natl. Acad. Sci. USA* **2008**, *105*, 18171.
- [10] M. Horie, K. Nishio, K. Fujita, S. Endoh, A. Miyauchi, Y. Saito, H. Iwahashi, K. Yamamoto, H. Murayama, H. Nakano, N. Nanashima, E. Niki, Y. Yoshida, *Chem. Res. Toxicol.* **2009**, *22*, 543.
- [11] E. J. Petersen, B. C. Nelson, *Anal. Bioanal. Chem.* **2010**, *398*, 613.
- [12] J. H. Park, G. von Maltzahn, E. Ruoslahti, S. N. Bhatia, M. J. Sailor, *Nat. Mater.* **2009**, *8*, 331.
- [13] X. Huang, J. Zhuang, X. Teng, L. Li, D. Chen, X. Yan, F. Tang, *Biomaterials* **2010**, *31*, 6142.
- [14] G. Bhabra, A. Sood, B. Fisher, L. Cartwright, M. Saunders, W. H. Evans, A. Surprenant, G. Lopez-Castejon, S. Mann, S. A. Davis, L. A. Hails, E. Ingham, P. Verkade, J. Lane, K. Heesom, R. Newson, C. P. Case, *Nat. Nanotechnol.* **2009**, *4*, 876.
- [15] T. Toshi, H. L. Ng, O. Bhattasali, T. Alber, E. C. Theil, *J. Am. Chem. Soc.* **2010**, *132*, 14562.
- [16] K. K. W. Wong, S. Mann, *Adv. Mater.* **1996**, *8*, 928.
- [17] M. Uchida, S. Kang, C. Reichhart, K. Harlen, T. Douglas, *Biochim. Biophys. Acta Gen. Subj.* **2010**, *1800*, 834.
- [18] L. B. Zhang, L. Laug, W. Münchgesang, E. Pippel, U. Gösele, M. Brandsch, M. Knez, *Nano Lett.* **2010**, *10*, 219.
- [19] C. D. San Martin, C. Garri, F. Pizarro, T. Walter, E. C. Theil, M. T. Nunez, *J. Nutr.* **2008**, *138*, 659.
- [20] S. Kalgaonkar, B. Lonnerdal, *J. Nutr. Biochem.* **2009**, *20*, 304.
- [21] R. Yu, P. M. Hinkle, *Mol. Endo.* **1998**, *12*, 737.
- [22] L. Wang, K. G. Rothberg, R. G. W. Anderson, *J. Cell Biol.* **1993**, *123*, 1107.
- [23] J. Wang, G. Yin, H. Liu, R. Li, R. L. Flemming, X. Sun, *J. Power Source* **2009**, *194*, 668.
- [24] I. Rousseau, S. Puntarulo, *Toxicology* **2009**, *264*, 155.
- [25] H. Wang, J. A. Joseph, *Free Radical Biol. Med.* **1999**, *27*, 612.
- [26] G. Balla, H. S. Jacob, J. Balla, M. Rosenberg, K. Nath, F. Apple, J. W. Eaton, G. M. Vercellotti, *J. Biol. Chem.* **1992**, *267*, 18148.
- [27] A. Cozzi, B. Corsi, S. Levi, P. Santambrogio, A. Albertini, P. Arosio, *J. Biol. Chem.* **2000**, *275*, 25122.
- [28] P. Arosio, S. Levi, *Biochim. Biophys. Acta Gen. Subj.* **2010**, *1800*, 783.
- [29] T. Xia, M. Kovochich, J. Brant, M. Hotze, J. Sempf, T. Oberley, C. Sioutas, J. I. Yeh, M. R. Wiesner, A. E. Nel, *Nano Lett.* **2006**, *6*, 1794.
- [30] Y. Liu, N. Hu, *Biosens. Bioelectron.* **2009**, *25*, 185.

Received: February 1, 2011  
Published online: April 28, 2011